Hindawi
Shock and Vibration
Volume 2022, Article ID 6554908, 14 pages
https://doi.org/10.1155/2022/6554908

Research Article

Influencing Mechanism of Detonator Location on Blasting Vibration with Electronic Initiation Technology

Junru Zhou, Dongwang Zhong, Lujun Cai, and Liang Wu

College of Science, Wuhan University of Science and Technology, Wuhan 430065, China

Correspondence should be addressed to Liang Wu; wuliang@wust.edu.cn

Received 30 September 2021; Accepted 10 January 2022; Published 7 April 2022

Academic Editor: Xiao Wang

Vibration velocity amplitude and frequency are the critical factors for assessing the adverse effects of blasting on surrounding structures. In this study, vibration signals were measured from a specially designed field test, in which blast holes were detonated by different initiation modes. Results of the field test indicate that the initiation mode has significant effects on blasting vibration. Then the influencing mechanism was revealed with the help of numerical simulation and theoretical analysis. Numerical simulation results show perfect accordance with filed test results. Five initiation modes to detonate the same explosion source, in descending orders of both velocity amplitude and vibration frequency, are the two initiation points, then the midpoint initiation and top and bottom initiation, followed by the bottom initiation and top initiation. By changing the location or increasing the number of detonators to reduce the length of subsource, the propagation path of detonation waves will be shrunk. Then the rising time of blast loading will be reduced and the rising rate will be accelerated, which lead to an increase in vibration frequency. In the meantime, the release and distribution of explosion energy will be accelerated unavoidably, which leads to an increase of vibration intensity. This study has considerable theoretical meaning and engineering value to guide for blasting construction.

1. Introduction

Drilling and blasting, as an essential rock mass excavation method, is frequently used in the construction of hydropower, mining, and municipal infrastructures [1–3]. Nowadays in order to implement precise-delay time control in blasting, the electronic initiation technology is widely adopted. The explosive charges in drilling and blasting are cylindrical with large length-to-diameter ratio. And the cylindrical charge in one blast hole is initiated by electronic detonators. Both the geometrical characteristics of cylindrical charge and the finite velocity of detonation have significant effects on the detonation reaction and after vibration field [4, 5]. Therefore, one thing to note is the layout of detonators in blasting design [6].

Many investigations, concerning the initiation location or detonation direction, have been carried out by various researchers [7]. Zhang conducted several experiments by changing the location of the detonation to increase the ore extraction efficiency [8]. Triviño and Mohanty analyzed the propagation of blasting waves under direct and reverse initiation modes and revealed the influence of initiation mode on the blasting seismic effect [9, 10]. Leng et al. compared the transmission mechanisms of the explosion energy between side-initiation and end-initiation modes and revealed the partition of the shock wave and the gas energy [11]. Many investigations have been finished about the effect of initiation mode on energy release, rock block casting, and rock breakage [12–14]. The blasting seismic effects are influenced by various factors, such as rock properties, blasting design parameters, explosive properties, and seismic wave propagation process [15–17]. Influencing mechanism of initiation mode on blasting vibration, however, is limited in the existing studies.

In this paper, investigation based on blasting source mechanism has been made to reduce seismic effects. Firstly, a field test was conducted to collect vibration signals under different initiation modes. Then with the help of numerical simulation, the effect of initiation mode on vibration frequency was investigated systematically. In the end, the

influence mechanism of initiation mode on vibration frequency was revealed by theoretical analysis.

2. Experimental Study

2.1. Experiments and Instrumentation. As shown in Figure 1(a), a series of single-hole blasting experiments were carried out in a geological survey tunnel. Field experiments included 12 vertical boreholes drilling on the tunnel floor. 2# rock emulsion explosive was adopted and the explosives per delay varied from 2.1 kg to 12 kg. Each borehole was initiated by nonelectric half-second detonator. Figure 1 describes the blasting design and the monitoring system and Table 1 lists all the parameters of blast experiment in detail. In Figure 1(b), 12 vertical boreholes were detonated by three initiation modes: top and bottom initiation mode, midpoint initiation mode, and bottom initiation mode. In top and bottom initiation mode, two detonators were placed closed to the top and bottom of charge length, respectively, and they were detonated simultaneously. In midpoint initiation mode, one detonator was placed in the middle of charge length. In bottom initiation mode, one detonator was put at the bottom of charge length.

The geology of the test site was generally at good condition. The topography was relatively flat. Vibration monitoring transducers, signature collecting, and logging devices and data processing system constituted the whole monitoring system. The blasting vibration was monitored by TC-4850 (Figure 2).

2.2. Experimental Results. In order to analyze the influence of the initiation mode on blasting vibration field, vertical boreholes in the field test were divided into four groups according to the hole depth. Blasting parameters in one group were supposed to be totally the same except the initiation mode. The vibration signal was recorded at monitoring points and then transformed to amplified-frequency spectra by fast Fourier transform. The recorded vibration data was analyzed in terms of both peak particle velocity and vibration frequency. Figure 3 gives a vibration signal induced by blast hole coding No. 2 and the process of spectrum analysis is given as well.

As shown in Figure 1 and Table 1, blast holes coding No. 1 and No. 2 were 8 m in depth. The initiation mode of No. 1 borehole was top and bottom initiated and the initiation mode of No. 2 borehole was bottom initiated. Vibration data induced by two blast holes versus distance from monitoring point to blast source are collected in Figure 4.

As the big dispersion in the dominant vibration frequency versus distance, the centroid vibration frequency is adopted in the analysis to compare the frequency content of signals intuitively [18]. Figure 5 shows the dominant vibration frequency and the centroid vibration frequency versus distance.

For the second group with 6 m and the third group with 4.5 m in depth, the initiation mode of No. 3 and 5 boreholes were middle initiated and the initiation mode of No. 4 and 6 boreholes were bottom initiated. The vibration amplitudes and frequency of the two groups are shown in Figures 6–9, respectively.

As shown in Figure 1, there are 6 vertical boreholes with 3 m in depth. Blast holes in the first row were middle initiated and boreholes in the second row were bottom initiated. However, according to the initiation sequence, the boundary condition of each hole is different (Figure 10). To eliminate the effect of boundary condition on blasting vibration, blast holes coding I-3 and II-1 were analyzed as one group, which is under the same boundary condition and initiated by different initiation mode. The vibration amplitude and frequency of the two blast holes are shown in Figures 11 and 12, respectively.

2.3. Experimental Result Analysis. In order to compare the effect of initiation mode on blasting vibration directly, some indices are defined by equations (1) and (2). The average frequency variation (GFV) and the average vibration amplitude variation (GAV) are used to quantify the global influence of initiation mode on blasting vibration. The maximum frequency difference (MFD) and the maximum vibration amplitude difference (MAD) are applied to quantify the most impacted level of initiation mode.

$$GFV = \int \left(\frac{f}{f_{bottom}} - 1 \right) dr, \tag{1a}$$

$$MFD = \max \left| \frac{f}{f_{bottom}} - 1 \right|, \tag{1b}$$

$$GAV = \int \left(\frac{PPV}{PPV_{bottom}} - 1 \right) dr, \tag{2a}$$

$$MAD = \max \left| \frac{PPV}{PPV_{bottom}} - 1 \right|, \tag{2b}$$

where r represents the distance from monitoring point to blast source; f and PPV are the centroid frequency and peak particle velocity of vibration induced by a certain initiation mode associated with each distance r, respectively. f_{bottom} and PPV_{bottom} are the centroid frequency and peak particle velocity of vibration induced by bottom initiation mode associated with each distance r, respectively. The traditional initiation mode, bottom initiation mode, is served as the control group.

In Table 2, the initiation mode has obvious influences on the seismic effect induced by single-hole blasting. The indices GAV and MAD indicate that vibration amplitude induced by top and bottom and midpoint initiation modes are higher compared with that induced by bottom initiation mode. The indices of vibration frequency GFV and MFD indicate that the vibration frequency will be increased by changing the bottom initiation to middle or top and bottom initiation. The global influencing index GFV shows a downward tendency with shortening the charge length, which means a limitation of the initiation influence on vibration frequency. And compared GAV with GFV, it can be

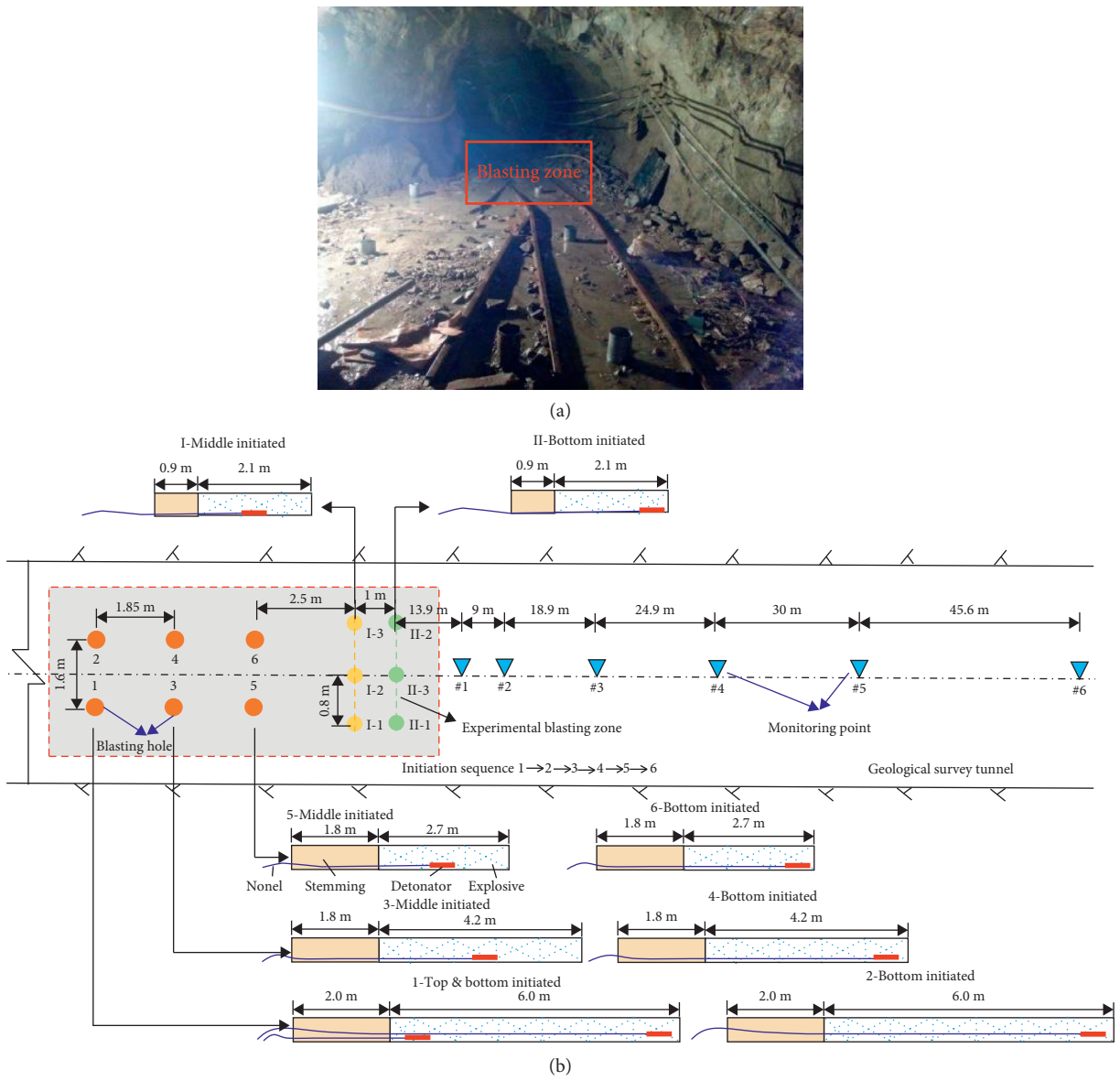

Figure 1: Field experiments. (a) Geology exploration tunnel. (b) Plan layout of blasting design and monitoring system.

Table 1: Parameters of vertical boreholes in the blast experiments.

Blast hole no.	Parameters of boreholes				Parameters of charge				Initiation mode
	Diameter (mm)	Depth (cm)	Hole pitch (cm)	Hole spacing (cm)	Diameter (mm)	Length (cm)	Stemming length (cm)	Charge per hole (kg)	
1	76	800	160	185	50	600	200	12.0	Top and bottom initiated
2	76	800	160	185	50	600	200	12.0	Bottom
3	76	600	160	185	50	420	180	8.4	Middle
4	76	600	160	185	50	420	180	8.4	Bottom
5	76	450	160	185	50	270	180	5.4	Middle
6	76	450	160	185	50	270	180	5.4	Bottom
I	42	300	80	100	32	210	90	2.1	Middle
II	42	300	80	100	32	210	90	2.1	Bottom

Figure 2: Blasting vibration intelligent monitor TC-4850 in the filed experiments.

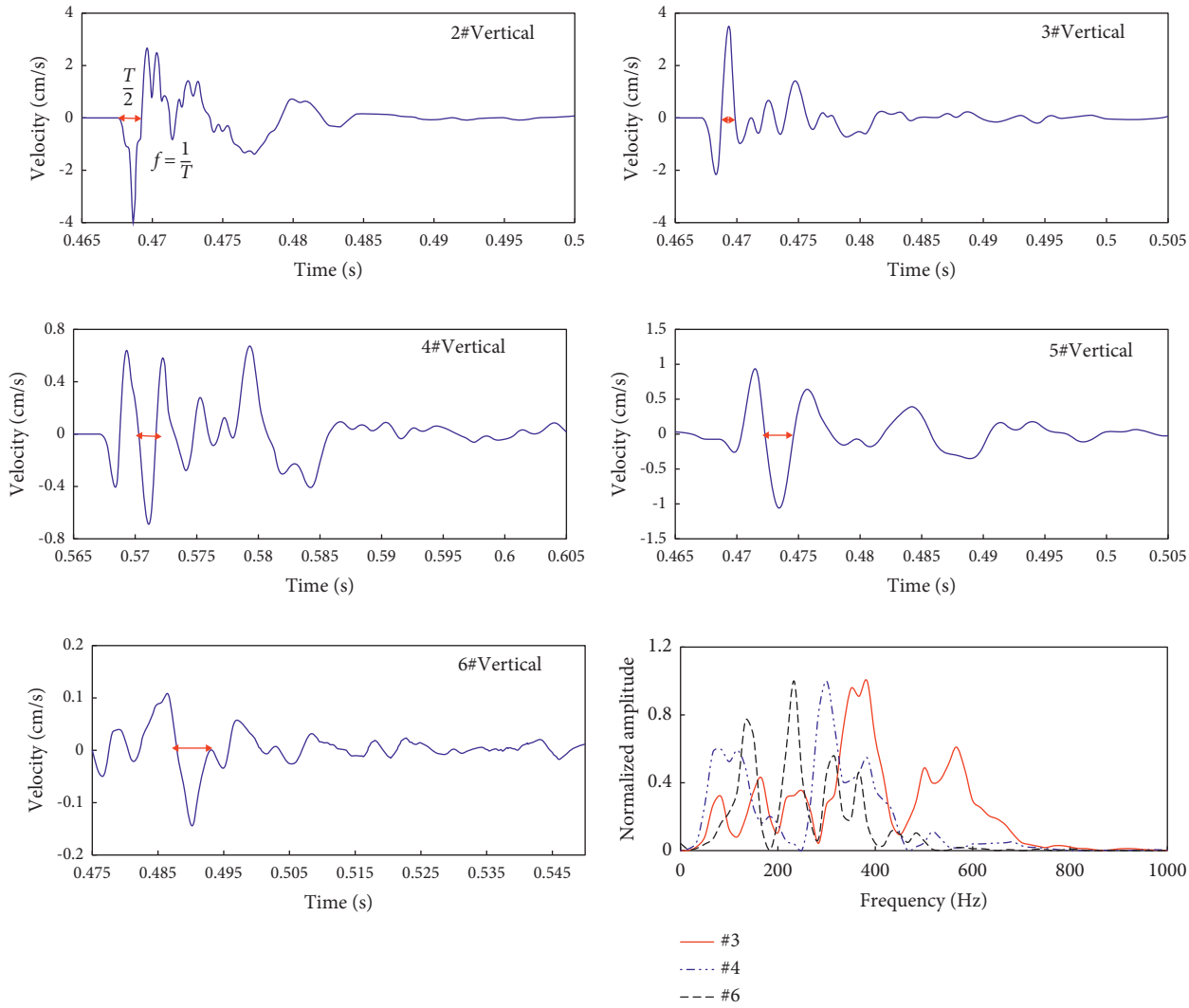

Figure 3: Vertical vibration of the second borehole blasting at different monitoring points.

concluded that the influence of initiation mode on vibration amplitude is more significant than that on vibration frequency. In summary, the vibration amplitude under bottom initiation mode is the highest compared with top and bottom and midpoint initiation mode. Vibration frequency will be increased by changing the location of initiation point from the bottom to the middle of charge length or by increasing the initiation point number.

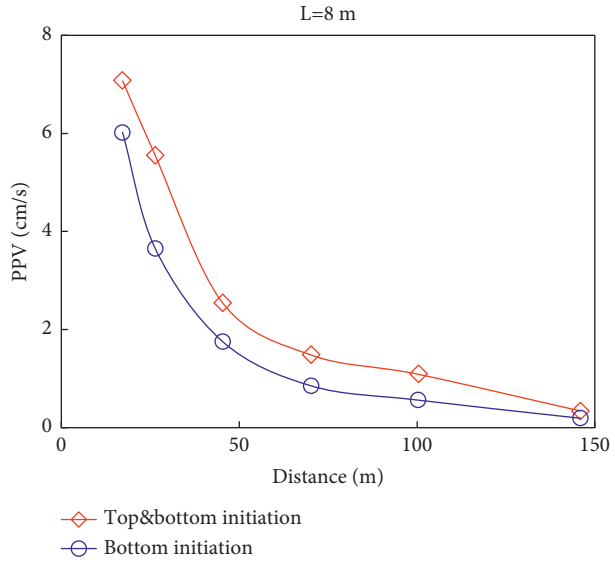

Figure 4: Peak particle velocity of the first group (two boreholes with 8 m in depth).

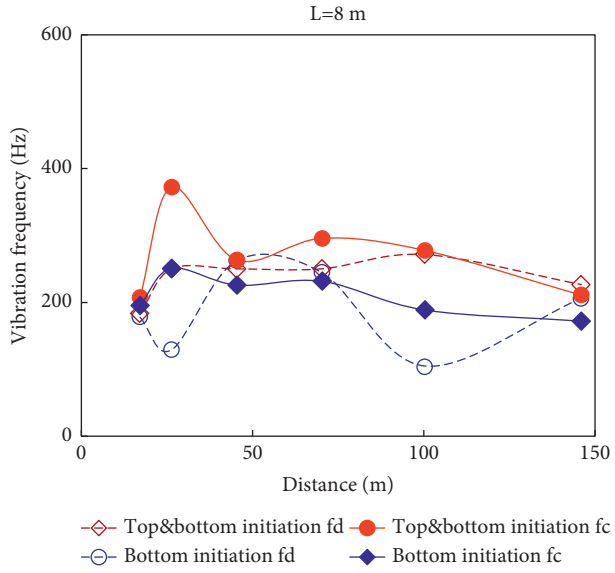

Figure 5: Vibration frequencies of the first group (boreholes with 8 m in depth).

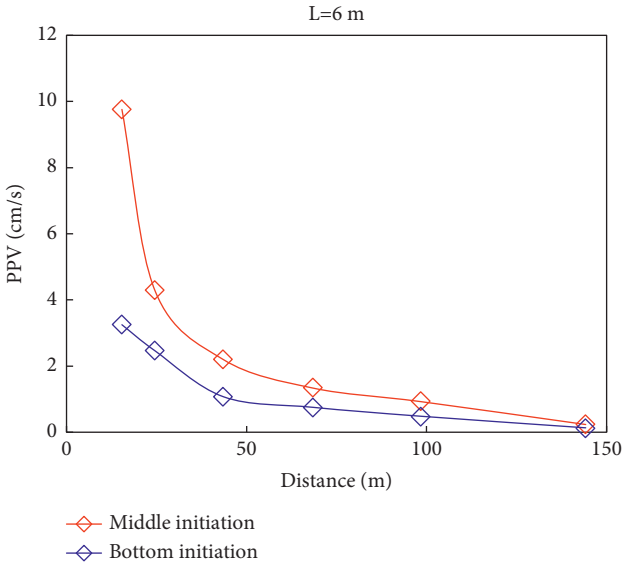

Figure 6: Peak particle velocity of the second group with 6 m in depth.

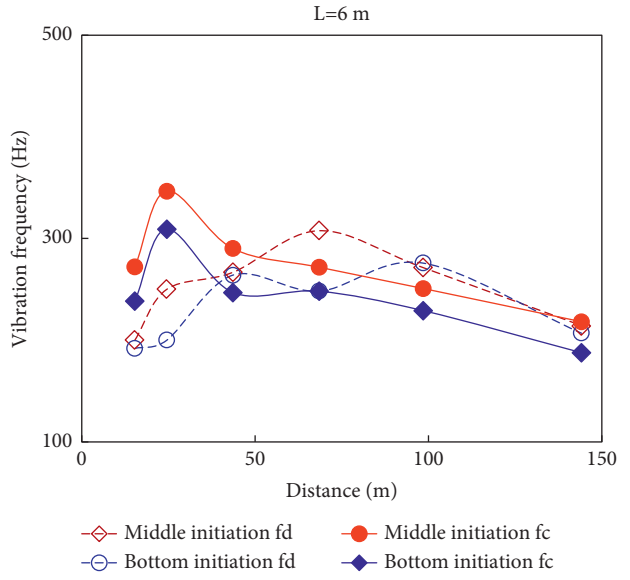

Figure 7: Vibration frequencies of the second group with 6 m in depth.

3. Numerical Simulation

As the complexity of the geological condition and the limitation of field experiment scale, the experimental data showed dispersed in a degree. Then numerical simulation by LS-DYNA was adopted to investigate the effect of initiation mode on vibration systematically as well as to verify the conclusion obtained from the field experiment.

3.1. Numerical Simulation Model. A single borehole blasting in semi-infinite rock mass was modeled in this section. The numerical model is briefly introduced as followed. Considered of symmetry, a quarter of the model was built. The rock model was a quarter of cylinder with 80 m in radius and 8 m in height. The length of borehole was 3 m totally with 2.1 m for charge and 0.9 m for stemming. The diameter of borehole was 42 mm. The diameter of charge was 30 mm. Transmitting boundary was applied on all the faces except the ground surface to simulate semi-infinite rock mass. Monitoring points were laid out on the ground surface (Test line). The numerical simulation model and the layout of monitoring points are shown in Figure 13.

MAT_HIGH_EXPLOSIVE_ BURN material model was used to describe explosive charge. Table 3 summarizes parameters of the explosive charge and the equation of state.

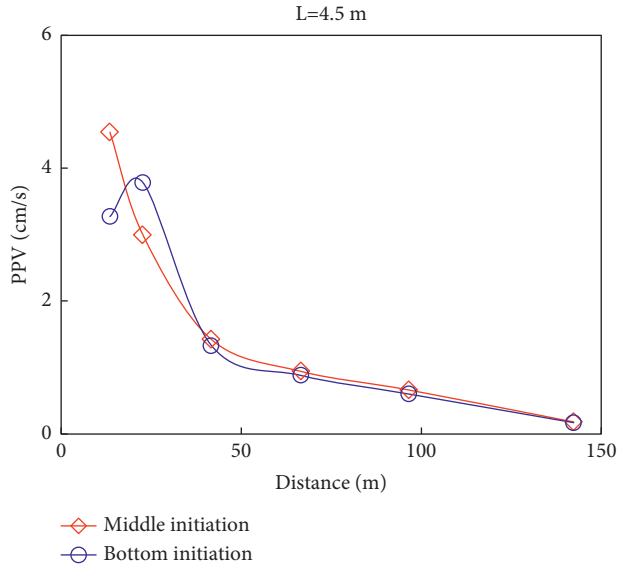

Figure 8: Peak particle velocity of the third group with 4.5 m in depth.

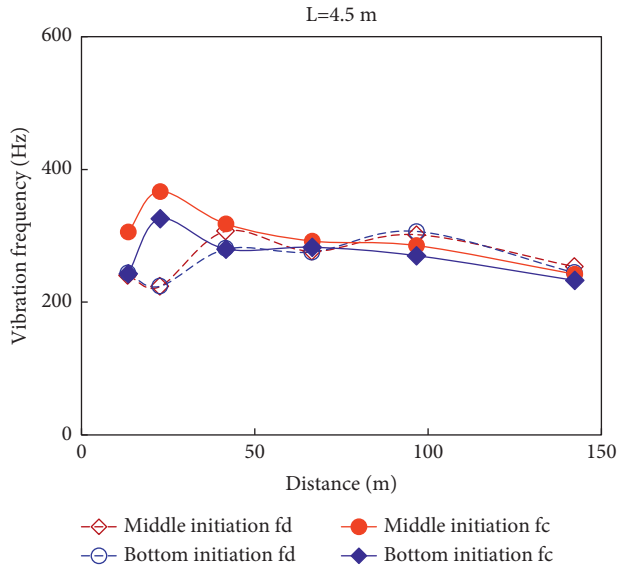

Figure 9: Vibration frequencies of the third group with 4.5 m in depth.

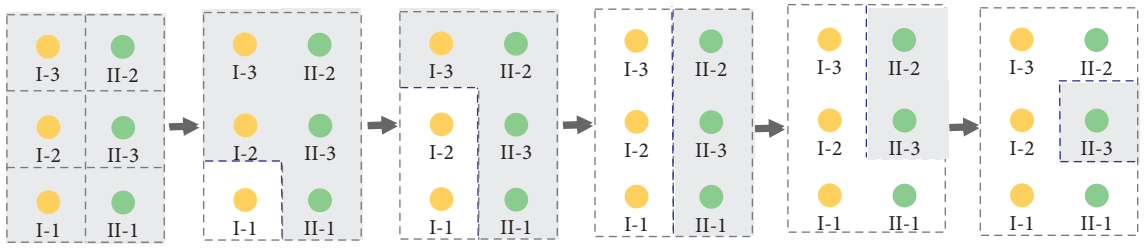

I-1: one free surface 1; I-2: two free surfaces; I-3: two free surfaces;
II-1: two free surfaces; II-2: three free surfaces; II-3: four free surfaces

Figure 10: The boundary condition of each hole during the initiation process.

MAT_PLASTIC_KINEMATIC material model was applied to simulate rock mass[19]. Parameters of rock model are listed in Table 4.

For air-decouple charge structure, MAT_NULL material model is used to simulate the air gap around charge. Parameters of air model are listed in Table 5.

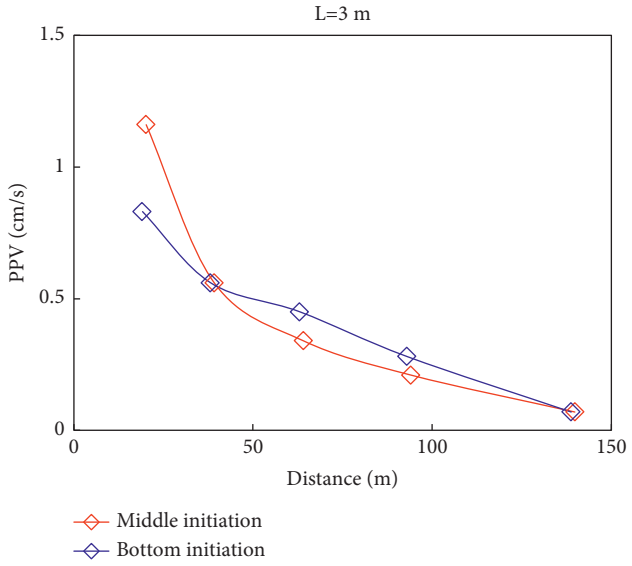

Figure 11: Peak particle velocity of two blast holes with 3 m in depth.

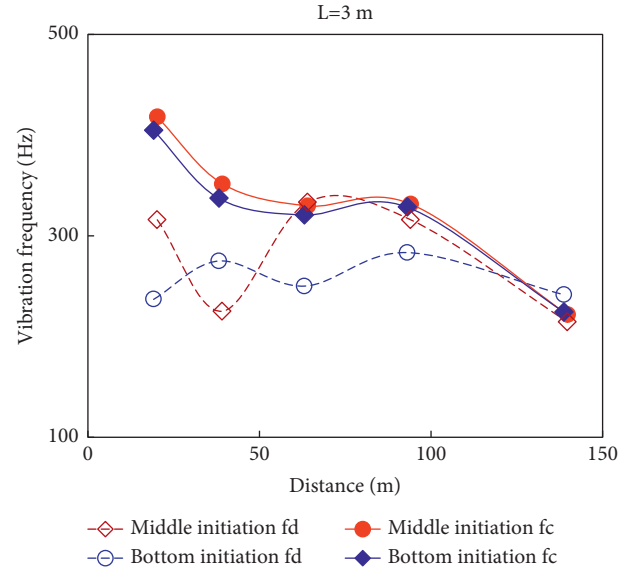

Figure 12: Vibration frequencies of two blast holes with 3 m in depth.

Table 2: Analysis data of influence of initiation mode on vibration signals.

Blasting condition	Vibration amplitude		Vibration frequency	
	GAV (%)	MAD	GFV (%)	MFD
$L = 8$ m with top and bottom initiation	35.04	0.95	32.09	0.48
$L = 6$ m with midpoint initiation	50.28	2.00	12.47	0.17
$L = 4.5$ m with midpoint initiation	−0.6	(−) 0.28	7.85	0.26
$L = 3$ m with midpoint initiation	5.68	0.33	1.97	0.04

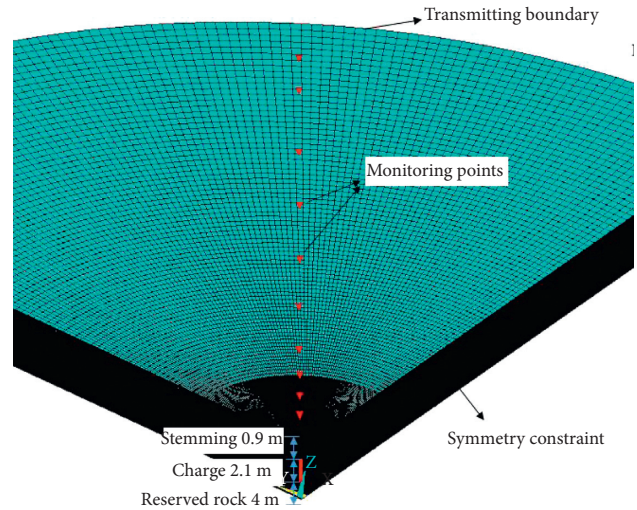

Figure 13: Numerical simulation model of drill blasting and the layout of test points.

3.2. Initiation Mode. Five initiation modes were applied to reveal the influence mechanism of initiation mode on blasting vibration: single initiation point located at the bottom, top and middle of charge, respectively, two initiation points located at the top and bottom of charge and detonated simultaneously, two initiation points located at the midpoint of half charge and detonated simultaneously (Figure 14).

3.3. Numerical Results Analysis. To avoid the effects caused by other factors, all the numerical model parameters were the same except the initiation mode. Vibration date induced by five initiation modes were collected and processed to frequency spectrum for frequency analysis in Figure 15.

The influencing indices of initiation location on seismic effect are summarized in Table 6 and Figures 16 and 17. Numerical simulation results indicate that the initiation location influences blasting vibration with regularity. As shown in Figure 17, various initiation modes to detonate the same explosion source, in descending order of velocity amplitude, are the two initiation points, followed by the midpoint initiation, top and bottom initiation, the bottom initiation, and the top initiation mode. Compared with bottom initiation mode, the vibration amplitude indices GAV and MAD of top initiation mode are −17.14% and −0.31, respectively, which means that the vibration magnitude monitored at ground surface is decreased. The GAVs of midpoint initiation and top and bottom initiation are different while both the MADs are 0.41. The GAV and MAD of two initiation points are 68.35% and 0.69, respectively, which means the highest vibration magnitude among the five initiation modes.

The initiation mode, in descending order of vibration frequency, is the two initiation points, then the midpoint initiation and top and bottom initiation, followed by the bottom initiation and top initiation. In Table 6, the GFV and MFD of top initiation mode are −0.94% and −0.14, respectively which approximate to zero. It means the

Table 3: Parameters of charge in numerical simulation.

Density (kg/m^3)	Velocity of detonation waves (m/s)	A (GPa)	B (GPa)	R_1	R_2	ω
1050	3850	209	3.5	5.8	1.29	0.39

Table 4: Parameters of rock in numerical simulation.

Density (kg/m^3)	Young's modulus (GPa)	Poisson's ratio	Yield strength (MPa)	Tangent modulus (GPa)
2750	60.5	0.22	70	36.2

Table 5: Parameters of air in numerical simulation.

Density (kg/m^3)	C_4	C_5	E_0	V_0
1.29	0.4	0.4	$0.25E+06$	1.0

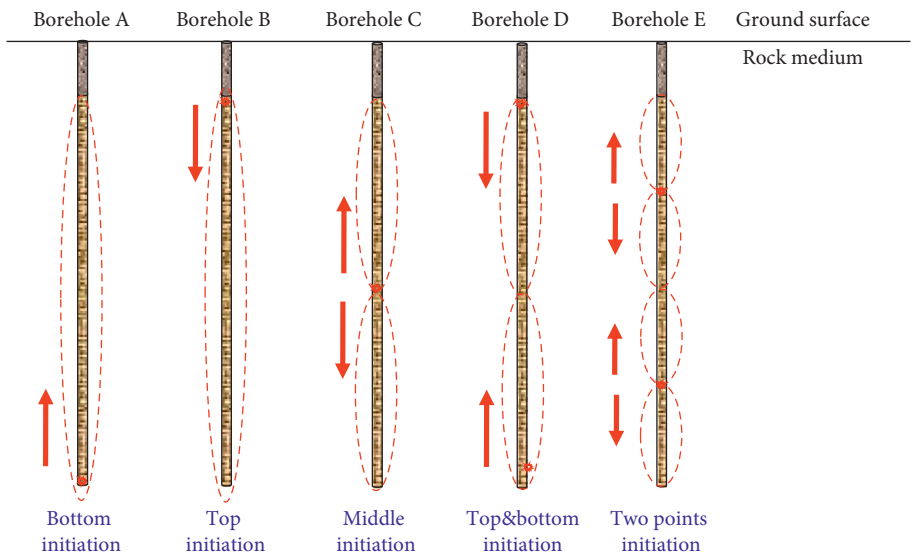

Figure 14: Five initiation modes in numerical analysis.

characteristic frequency of vibration detonated by top initiation is very similar to that detonated by bottom initiation mode. For midpoint initiation mode, the GFV and MFD are 28.90% and 0.27, respectively. For top and bottom initiation mode, the GFV and MFD are 31.10% and 0.28, respectively. The indices of vibration frequency of midpoint initiation and top and bottom initiation show similar values. And the GFV and MFD of two initiation points are 40.20% and 0.32, respectively, which indicate that vibration frequency detonated by two initiation points are the highest.

And compared GAV with GFV, it can be concluded that the influence of initiation mode on vibration amplitude is more significant than on vibration frequency. In summary, vibration amplitude and frequency will be increased by changing the location of initiation point from the bottom to the middle of charge length or by increasing the initiation points. By changing the location or increasing the number of initiation points, the whole explosion source is divided into several subsource initiated by each detonator simultaneously. To shorten the length of subexplosion source, the vibration amplitude and frequency increase in some degree. Moreover, compared bottom initiation and top initiation mode, the propagation direction of the detonation wave influences the vibration amplitude in the meantime.

4. Influencing Mechanism of Initiation Mode on Seismic Vibration

In summary, by changing the location or the number of initiation points to reduce the length of subsource, the vibration frequency and velocity amplitude will be increased. Two main factors may explain this phenomenon: the superposition of detonation waves inspired by each subsource and the propagation path of the detonation wave.

As shown in Figure 14, the initiation point at the bottom of charge means the detonator will initiate the whole charge and the detonation wave is supposed to propagate from the bottom to the top. The initiation point at the top of charge means the detonator will initiate the whole charge as well and the detonation wave is supposed to propagate from the top to the bottom. For midpoint initiation mode or top and bottom initiation mode, the location of detonators in the charge means dividing the whole explosion source into two subsources with half

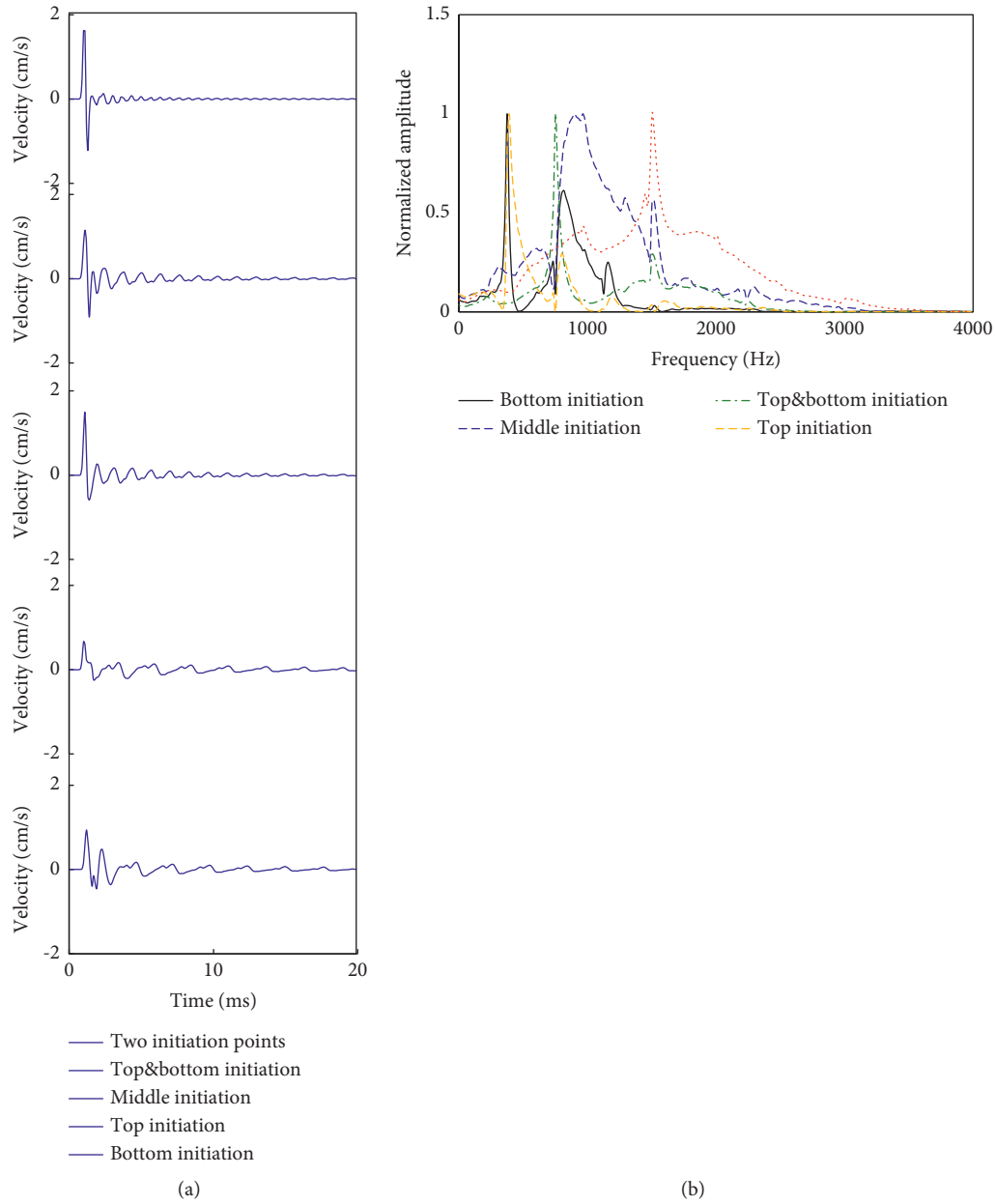

Figure 15: Vibration signals at $r = 5$ m induced by 5 initiation modes. (a) Vibration history. (b) Normalized amplitude spectrum.

Table 6: Vibration increments of different initiation modes in numerical simulation.

Blasting condition	Vibration amplitude		Vibration frequency	
	GAV (%)	MAD	GFV (%)	MFD
Top initiation	−17.14 (↓)	−0.31 (↓)	−0.94 (↓)	−0.14 (↓)
Midpoint initiation	50.81	0.41	28.90	0.27
Top and bottom initiation	35.08	0.41	31.10	0.28
Two initiation points	68.35	0.69	40.20	0.32

whole charge length. The two subsources are detonated simultaneously. For middle initiation, the detonation waves are supposed to propagate from the middle to the top and bottom while for top and bottom initiation mode, the detonation waves propagate from the top and bottom to the middle at the same time. For initiation mode with two detonators, the whole explosion source is divided into four same subsources with a quarter of whole charge length. The four subsources are detonated simultaneously by two detonators. And the direct propagation path of the

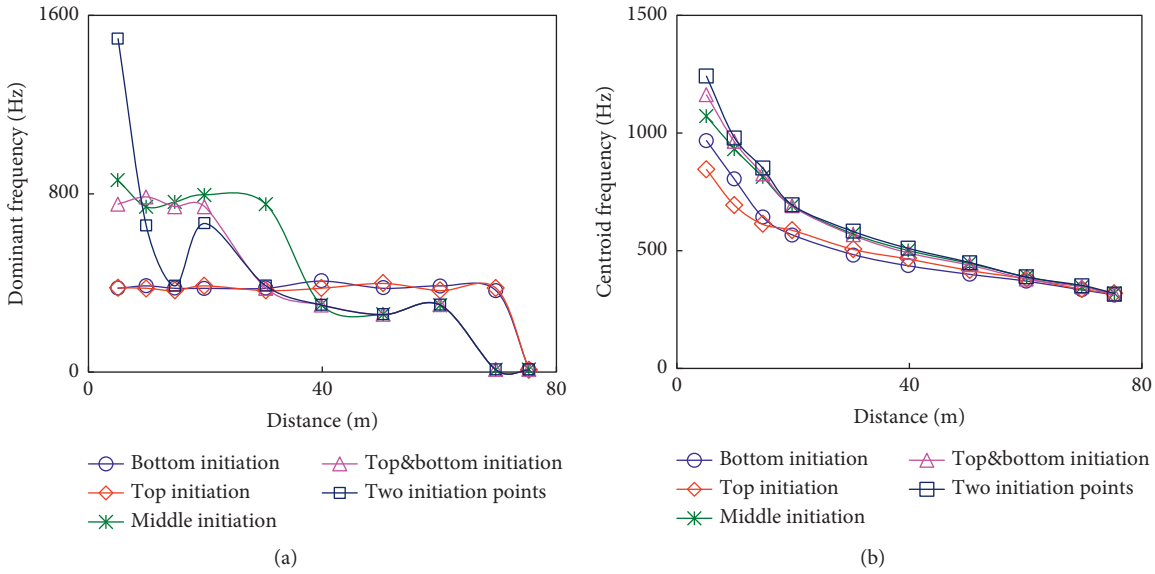

Figure 16: Vibration frequency versus distance induced by five initiation modes. (a) Dominant frequency. (b) Centroid frequency.

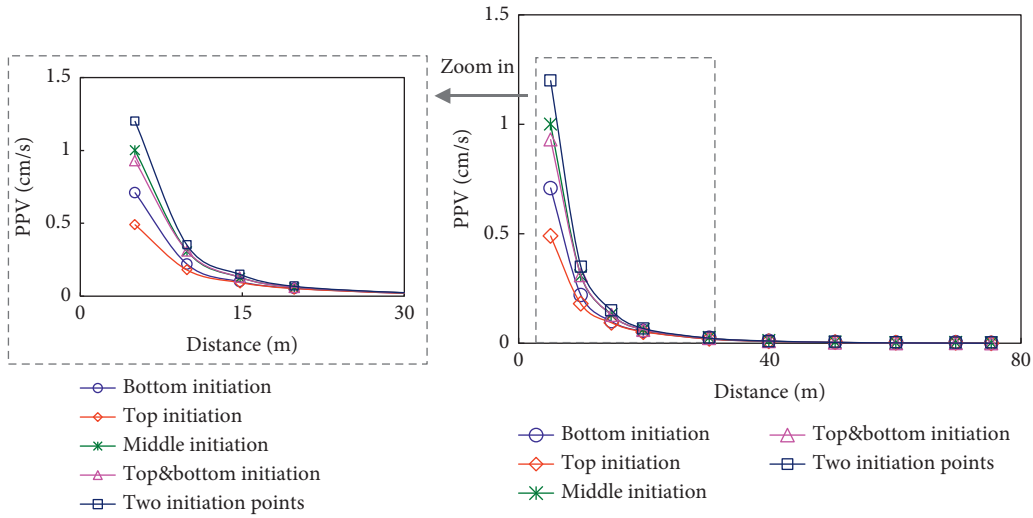

Figure 17: Peak particle velocity of longitudinal components in numerical simulation.

detonation wave induced by each detonator is a quarter of the whole charge length.

4.1. Effects on Frequency Spectrum. An expression of vibration amplitude spectrum is derived by Zhou et al. [5] for analyzing the characteristic frequencies of vibration induced by a spherical charge exploding in an infinite viscoelastic medium.

$$F_n(\omega) = \frac{\exp\left(-\omega r/2Q_r V_p\right)\left|S_\sigma(j\omega)\right| r_e V_p \omega \sqrt{V_p^2 + r^2\omega^2/4\mu r^2}}{\sqrt{\left(V_p/r_e\right)^4 + \left[1 - (\lambda + 2\mu)/(2\mu)\right]\left(V_p/r_e\right)^2\omega^2 + \left[(\lambda + 2\mu)/(4\mu)\right]^2\omega^4}}, \quad (3)$$

where $F_n(\omega)$ is the frequency spectrum of vibration in viscoelastic media. $S_\sigma(j\omega)$ is the complex spectrum of blasting load $\sigma(\tau)$. ω is the angular frequency. r_e is the equivalent radius of spherical charge. r is the distance from blast source to monitoring point. ρ is the density of elastic isotropic propagation medium. λ and μ are the Lame coefficients of propagation medium. V_p is the longitudinal wave velocity, $V_p = \sqrt{\lambda + 2\mu/\rho}$. Q_r is the geology quality factor.

As indicated in (3), three important indexes are defined to describe the blasting load: the peak value of the blasting load, the duration of the blasting load, and the load rising time. And the load rising time is the main influencing factor of vibration frequency.

The blasting load acting on the equivalent elastic boundary is simplified as (4) [20]. After Fourier transformation, the blasting load history turned to the Fourier amplitude-frequency spectrum as in (5).

$$\sigma(t) = \begin{cases} 0, & t < -\tau_1; \\ \sigma_{\max}\left(1 + t/\tau_1\right), & -\tau_1 \le t \le 0; \\ \sigma_{\max}\left(1 - t/\tau_2\right), & 0 \le t \le \tau_2; \\ 0, & t > \tau_2; \end{cases} \tag{4}$$

$$\left|S_\sigma(\omega)\right| = \frac{\sigma_{\max}}{a_e b_e \tau \omega^2}\left[1 + a_e^2 + b_e^2 + 2a_e b_e \cos\,\omega\tau - 2\left(a_e \cos\, b_e \omega\tau + b_e \cos\, a_e \omega\tau\right)\right]^{1/2}, \tag{5}$$

where $\sigma_{\max}$ is the peak value of the blasting load, τ is the duration of the blasting load, τ_1 is the load rising time, and τ_2 is the load decreasing time, $a_e = \tau_1/\tau$, $b_e = \tau_2/\tau$.

The effect of the load rising process on load frequency spectrum is investigated by numerical calculation of (5). τ_1 is set as the control variable to reveal the influence mechanism of the load rising time. Parameters are introduced in the following analysis: $\sigma_{\max} = 30$ MPa, $\tau = 10$ ms. The load frequency spectrum was calculated with different τ_1 ranging from 1 to 5 ms. Results are shown in Figure 18. In order to better compare the change of amplitude spectra, Figure 18 uses the ratio of amplitude to the maximum amplitude to substitute the original amplitude as Y-axis. It reveals that by shortening the rising time of blasting load, the load rising rate is accelerated, the spectrum amplitude corresponding to high frequency increases, and the proportion of seismic energy in higher frequency band to total energy increases.

The process of blasting loads acting on the blast hole were monitored at 6 points coding from 1# to 6# placed along the borehole in the numerical simulation model (Figure 19). The load rising time and rising rate of each monitoring point under different initiation modes were extracted in Figure 20 to reveal the influence mechanism of initiation mode on the load rising process.

For bottom initiation mode and top initiation mode in Figure 14, the propagation of detonation waves are very similar only except the spatial propagation direction. The load rising time and rising rate of bottom initiation are identical with top initiation mode. As shown in Figure 20, the load rising times of both bottom initiation and top initiation are longest, and the rising rates are the lowest in five initiation modes which means the minimum proportion of seismic energy in higher frequency band. Therefor the blasting vibration frequencies initiated by single detonator placed in the top or bottom of charge are lowest in the five initiation modes then followed by the midpoint initiation and top and bottom initiation. For initiation with two detonators, the load rising time is shortest and the rising rate is fastest which indicates the maximum seismic energy in high frequency band. Therefore vibration frequency is highest.

The results of this study demonstrated that there is definite relationship in the initiation mode and the vibration frequency. The initiation mode determines the propagation path of the detonation wave. By changing the location or the number of initiation point to reduce the charge length of subsource, the load rising time shrinks. Then the characteristic frequencies increase in some degree.

4.2. Effect on Vibration Velocity Amplitude. As shown in Figure 17, various initiation modes to detonate the same explosion source, in descending order of velocity amplitude, are the two initiation points, followed by the midpoint initiation, top and bottom initiation, the bottom initiation, and the top initiation mode.

In Figure 15, five initiation modes to detonate the same explosion source, in ascending order of the width of vibration time interval, are the two initiation points, the midpoint initiation and top and bottom initiation, followed by the bottom initiation and the top initiation mode. Figure 21 lists the time-kinetic energy densities under five initiation modes. For initiation with two detonators, the kinetic energy is the largest and its corresponding time domain is the narrowest then followed by the midpoint initiation and top and bottom initiation. The time domains of top initiation mode and bottom initiation mode are the broadest while there is an obvious difference in values of the kinetic energy.

The blast stress field of a cylindrical charge is not uniformly distributed, but strengthened along the propagation direction of the detonation wave, which is caused by the phase delay effect of the element charges. The inherent mechanism lies in the geometric characteristic of the charge (cylindrical shape) and the finite VOD of the explosive. For bottom initiation mode with the detonator placed at the bottom (Borehole A), the detonation waves propagate upwards the borehole and the explosive energy is transmitted to the ground surface. As the explosion energy is preferentially transmitted to the upper rock mass under bottom

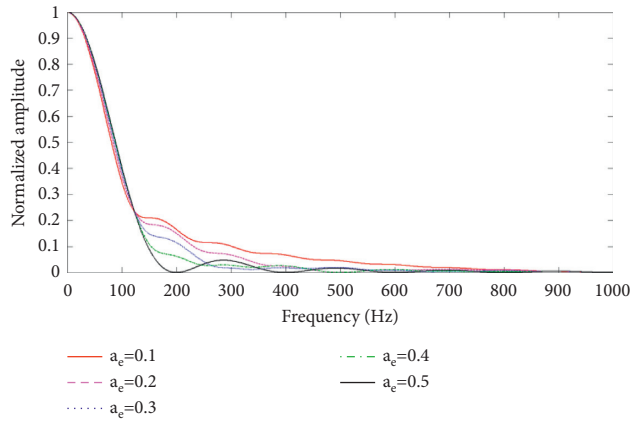

Figure 18: Normalized amplitude spectra of blasting load with different rising times.

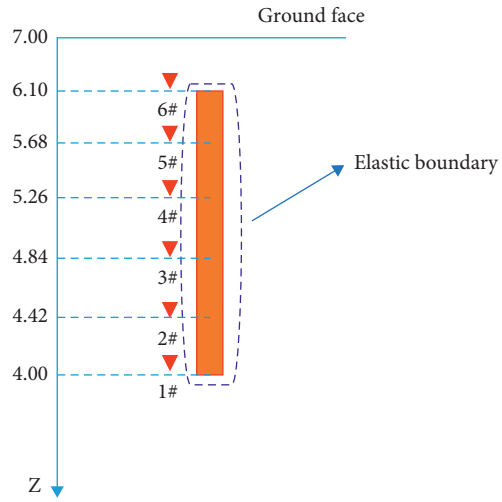

Figure 19: Layout of monitoring points along borehole to monitor explosion pressure.

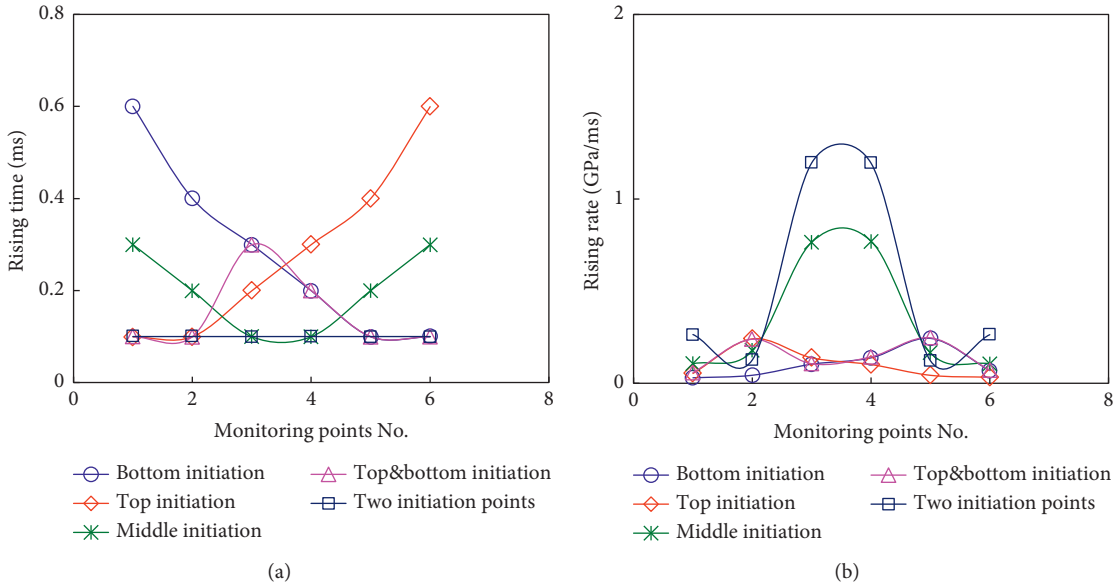

Figure 20: Rising process of pressure at monitoring points under different initiation modes. (a) Rising time. (b) Rising rate.

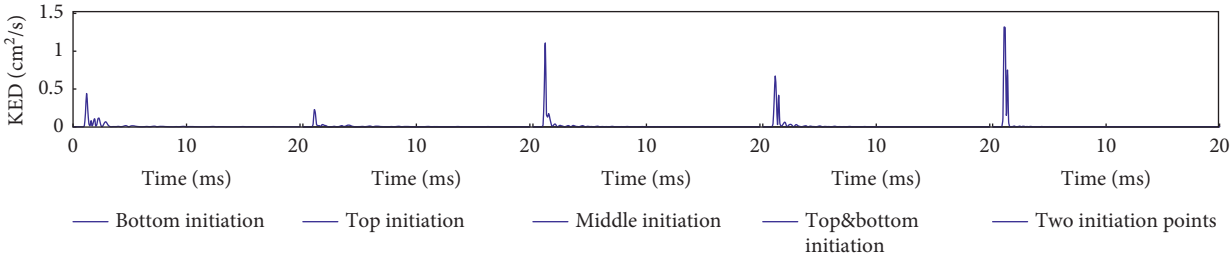

Figure 21: Kinetic energy densities (KED) under five initiation modes.

initiation, the seismic effects of ground surface is stronger than that under top initiation (Borehole B).

As was stated above, the influencing mechanism of initiation mode on the vibration velocity can be explained from two aspects: (1) the release rate of explosion energy is closely associated with the initiation points. (2) The spatial distribution of explosive energy is determined by the propagation direction of detonation waves.

5. Discussions

During rock blasting, the initiation mode plays an important role in breakage profile, seismic effect, and fragmentation effect. Therefore, available initiation mode should be determined due to different emphases of each engineering. The present study aims to reveal the seismic effects under different initiation modes and each initiation mode has its own advantages and disadvantages. Initiation modes to detonate the same explosion source, in descending order of both velocity amplitude and vibration frequency, are the two initiation points, followed by the midpoint initiation, top and bottom initiation, the bottom initiation, and the top initiation mode. From the vibration frequency point of view, by shortening the subsource length, the blasting vibration frequency will be increased which means beneficial to the control of blasting seismic effects. While from the velocity amplitude point of view, by shortening the subsource length, the blasting vibration amplitude will be strengthened, which is against controlling blasting adverse effects.

As was stated above, there is no best initiation mode that is suitable for all situations, and sharp conflicts will arise if both aspects are considered. The initiation location should be changed according to the on-site situations, so as to effectively reduce the hazards of blasting as much as possible. If the protecting objects are close to blasting zone, the vibration amplitude should be controlled in a strict way. Then the vibration velocity is the most important index for initiation mode selection. If the protecting objects are far away from the blasting zone and inclined to resonate during blasting, then the vibration frequency is the critical index for initiation mode selection.

Many other influence factors, such as the blasting parameters, the explosive properties, the drilling parameters, and the layout of boreholes can never be ignored in rock blasting, which were not covered in the present study. Further investigation will be conducted in the next stage.

6. Conclusions

In the present study, the seismic effects of initiation mode were investigated both numerically and experimentally. And the influencing mechanism was revealed theoretically. Some useful conclusions can be drawn as follows:

(1) Initiation mode plays an important role in seismic effect induced by rock blasting. Five initiation modes to detonate the same explosion source, in descending orders of both velocity amplitude and frequency, are the two initiation points, then the midpoint initiation and top and bottom initiation, followed by the bottom initiation and top initiation.

(2) The influencing mechanism of initiation mode on vibration frequency is revealed. The location of detonators in one cylindrical charge means dividing the whole explosion source into several subsources initiated simultaneously. By changing the location or increasing the number of detonators to reduce the length of subsource, the propagation path of detonation waves will be shrunk. Then, the rising time of blast loading will be reduced and the rising rate will be accelerated, which lead to an increase in vibration frequency.

(3) The influencing mechanism of initiation mode on the vibration velocity can be explained from two aspects. Firstly, the release rate of explosion energy is closely associated with the initiation points. Secondly, the spatial distribution of explosive energy is determined by the propagation direction of detonation waves.

Each initiation mode has its own advantage and disadvantage. The appropriate location of detonators should be designed according to the onsite situation.

Data Availability

Basic data can be obtained from the corresponding author when needed.

Conflicts of Interest

The authors declare that they have no conflicts of interest.

Acknowledgments

This work was supported by Chinese National Natural Science Foundation (51909196) and Open Fund of Key Lab

of Rock Mechanics in Hydraulic Structural Engineering, Ministry of Education (RMHSE1904). The authors wish to express their thanks to all supporters.

References

[1] X. P. Li, J. H. Huang, Y. Luo, and P. P. Chen, "A study of smooth wall blasting fracture mechanisms using the Timing Sequence Control Method," *International Journal of Rock Mechanics and Mining Sciences*, vol. 92, pp. 1–8, 2017.

[2] S. Y. Xiao, L. J. Su, Y. J. Jiang, and Z. X. Liu, "Numerical analysis of hard rock blasting unloading effects in high in situ stress fields," *Bulletin of Engineering Geology and the Environment*, vol. 78, no. 6, pp. 1–9, 2017.

[3] E. Ebrahimi, M. Monjezi, M. R. Khalesi, and D. J. Armaghani, "Prediction and optimization of back-break and rock fragmentation using an artificial neural network and a bee colony algorithm," *Bulletin of Engineering Geology and the Environment*, vol. 75, no. 1, pp. 27–36, 2016.

[4] C. H. Dowding, *Blast Vibration Monitoring and Control Vol 297*, Prentice-Hall Englewood Cliffs, 1985.

[5] J. Zhou, W. Lu, P. Yan, M. Chen, and G. Wang, "Frequency-dependent attenuation of blasting vibration waves," *Rock Mechanics and Rock Engineering*, vol. 49, no. 10, pp. 4061–4072, 2016.

[6] X. Qiu, X. Shi, Y. Gou, J. Zhou, H. Chen, and X. Huo, "Short-delay blasting with single free surface: results of experimental tests," *Tunnelling and Underground Space Technology*, vol. 74, pp. 119–130, 2018.

[7] B. P. Zhang, Q. M. Zhang, and F. L. Huang, *Detonation Physics*, Weapon Industry Press, Beijing, (In Chinese), 2001.

[8] Z. Zhang, "Increasing ore extraction by changing detonator positions in lkab malmberget mine," *Fragblast*, vol. 9, no. 1, pp. 29–46, 2005.

[9] L. F. Triviño, B. Mohanty, and B. Milkereit, "Seismic waveforms from explosive sources located in boreholes and initiated in different directions," *Journal of Applied Geophysics*, vol. 87, pp. 81–93, 2012.

[10] I. A. Onederra, J. K. Furtney, E. Sellers, and S. Iverson, "Modelling blast induced damage from a fully coupled explosive charge," *International Journal of Rock Mechanics and Mining Sciences*, vol. 58, no. 58, pp. 73–84, 2013.

[11] Z. D. Leng, W. B. Lu, M. Chen, Y. Fan, Y. Peng, and G. Wang, "Explosion energy transmission under side initiation and its effect on rock fragmentation," *International Journal of Rock Mechanics and Mining Sciences*, vol. 86, pp. 245–254, 2016.

[12] L. Liu, M. Chen, W. Lu, Y. Hu, and Z. Leng, "Effect of the location of the detonation initiation point for bench blasting," *Shock and Vibration*, vol. 2015, no. 7, pp. 1–11, 2015.

[13] B. Zhu, N. Jiang, C. Zhou, X. Luo, Y. Yao, and T. Wu, "Dynamic failure behavior of buried cast iron gas pipeline with local external corrosion subjected to blasting vibration," *Journal of Natural Gas Science and Engineering*, vol. 88, p. 103803, 2021.

[14] Q. Gao, W. Lu, Z. Leng, Z. Yang, Y. Zhang, and H. Hu, "Effect of initiation location within blasthole on blast vibration field and its mechanism," *Shock and Vibration*, vol. 2019, pp. 1–18, Article ID 5386014, 2019.

[15] H. Li, X. Li, J. Li, X. Xia, and X. Wang, "Application of coupled analysis methods for prediction of blast-induced dominant vibration frequency," *Earthquake Engineering and Engineering Vibration*, vol. 15, no. 1, pp. 153–162, 2016.

[16] A. Karadogan, A. Kahriman, and U. Ozer, "A new damage criteria norm for blast-induced ground vibrations in Turkey," *Arabian Journal of Geosciences*, vol. 7, no. 4, pp. 1617–1626, 2014.

[17] N. Jiang, C. Zhou, S. Lu, and Z. Zhang, "Effect of underground mine blast vibrations on overlaying open pit slopes: a case study for daye iron mine in China," *Geotechnical & Geological Engineering*, vol. 36, no. 4, pp. 1–15, 2017.

[18] J. H. Yang, W. B. Lu, Q. H. Jiang, C. Yao, and C. B. Zhou, "Frequency comparison of blast-induced vibration per delay for the full-face millisecond delay blasting in underground opening excavation," *Tunnelling and Underground Space Technology*, vol. 51, pp. 189–201, 2016.

[19] Y. Hu, W. Lu, X. Wu, M. Liu, and P. Li, "Numerical and experimental investigation of blasting damage control of a high rock slope in a deep valley," *Engineering Geology*, vol. 237, pp. 12–20, 2018.

[20] O. Yilmaz and T. Unlu, "Three dimensional numerical rock damage analysis under blasting load," *Tunnelling and Underground Space Technology*, vol. 38, no. 9, pp. 266–278, 2013.